

Rotation of the magnetic easy axis in $\text{La}_{0.67}\text{Sr}_{0.33}\text{MnO}_3$ thin film on $\text{NdGaO}_3(112)$

Hiroaki Nishikawa,^{1,2} Evert Houwman,^{2,a)} Hans Boschker,² Mercy Mathews,² Dave H. A. Blank,² and Guus Rijnders^{2,b)}

¹School of Biology-Oriented Science and Technology, Kinki University, 930 Nishi-Mitani, Kinokawa, Wakayama 649-6493, Japan

²MESA+ Institute for Nanotechnology, University of Twente, 7500 AE Enschede, The Netherlands

(Received 21 July 2008; accepted 5 January 2009; published online 26 January 2009)

The in-plane magnetic anisotropy is studied for pseudocubic $\{011\}_{\text{pc}}$ oriented $\text{La}_{0.67}\text{Sr}_{0.33}\text{MnO}_3$ (LSMO) thin film grown on orthorhombic $\text{NdGaO}_3(\text{NGO})(112)_o$ (the subindices “pc” and “o” indicate the pseudocubic and orthorhombic lattice structure, respectively). The direction of the in-plane remanent magnetization of LSMO thin films with different thicknesses is determined. With increasing film thickness the easy axes rotate and the anisotropy changes from uniaxial to biaxial. This is associated with the increasing symmetry of the LSMO with increasing thickness, starting with a monoclinic LSMO structure at the nonrectangular $\text{NGO}(112)_o$ surface unit cell of the substrate, developing into an orthorhombic structure at the top part of the thickest films. © 2009 American Institute of Physics. [DOI: 10.1063/1.3074445]

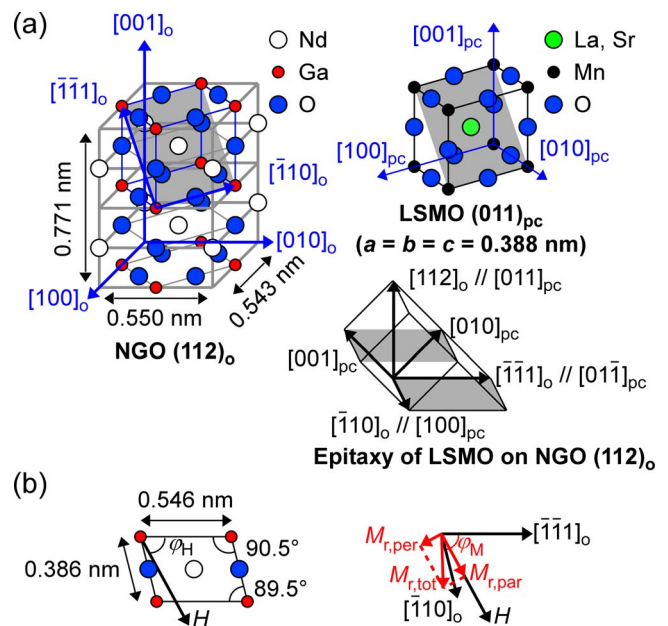
Manganites such as $\text{La}_{0.67}\text{Sr}_{0.33}\text{MnO}_3$ (LSMO) are of great interest because of their colossal magnetoresistance^{1,2} and the predicted full spin polarization.³ In practice the very high tunneling magnetoresistance (TMR) ratios, expected from the full spin polarization, is rarely obtained and TMR vanishes at much lower temperature than the LSMO Curie temperature.⁴⁻⁶ One of the possible causes of this problem is the so-called “magnetic dead layer” at interfaces with other perovskites. An important reason is believed to be charge transfer.^{6,7} In order to suppress the interface doping, $\{011\}_{\text{pc}}$ oriented growth of LSMO may be a solution⁸ (the subindices “pc,” “c,” and “o” indicate the pseudocubic, cubic, and orthorhombic lattice structures, respectively). In that case the perovskite ABO_3 is composed of stacked $(\text{ABO})^{4+}$ and $(\text{O}_2)^{4-}$ layers, irrespective of the cation valence states, throughout the LSMO electrode and the barrier layers. For the very high TMR ratios, other issues to be resolved are the magnetization properties and magnetic domain structure of the LSMO electrodes. To this end we are investigating the relationships between the strain state, the structure change, and the magnetic anisotropy of the LSMO grown on various substrates. There are several substrates available to prepare $\{011\}_{\text{pc}}$ oriented LSMO thin films, for example, $\text{STO}(011)_c$, $\text{NGO}(100)_o$, $\text{NGO}(010)_o$, as well as $\text{NGO}(112)_o$.

Here, we report on the magnetic anisotropy of $\{011\}_{\text{pc}}$ oriented LSMO thin films of various thicknesses grown on $\text{NGO}(112)_o$ substrates. It is shown that with increasing film thickness the magnetic anisotropy changes from an essentially uniaxial magnetic easy axis to biaxial.

Figure 1(a) shows the $\text{NGO}(112)_o$ plane in the orthorhombic unit cell of NGO, as well as the $(011)_{\text{pc}}$ plane in the pseudocubic unit cell of LSMO, which can be stacked epitaxially on $\text{NGO}(112)_o$. The two lattice vectors defining the $\text{NGO}(112)_o$ surface unit are: $\text{NGO}[\bar{1}\bar{1}1]_o$, corresponding to $\text{LSMO}[01\bar{1}]_{\text{pc}}$ and $\text{NGO}[\bar{1}10]_o$, equivalent to $\text{LSMO}[100]_{\text{pc}}$.

The lattice mismatch in both directions is compressive for LSMO thin films, with -0.59% along $[\bar{1}\bar{1}1]_o$ and -0.47% along $[\bar{1}10]_o$. An important feature of the $\text{NGO}(112)_o$ surface is the nonrectangular symmetry as shown in Fig. 1(b), which implies that the $(011)_{\text{pc}}$ surface plane of the LSMO pseudocube, as well as the $(001)_{\text{pc}}$ and $(010)_{\text{pc}}$ side faces have a long and a short diagonal.

$\text{NGO}(112)_o$ single crystals were annealed at 950°C for 1 h in 1 bar O_2 flow to prepare atomically smooth substrates, as was confirmed by atomic force microscopy. LSMO thin films were deposited by the pulsed laser deposition technique



Surface asymmetry of $\text{NGO}(112)_o$ In-plane magnetization

FIG. 1. (Color online) (a) Schematic of the $\text{NGO}(112)_o$ surface and its epitaxial relationship with the $\text{LSMO}(011)_{\text{pc}}$ surface. (b) Top view of the surface unit cell of the $\text{NGO}(112)_o$. The angle of the applied magnetic field (φ_H) is defined.

^{a)}Electronic mail: e.p.houwman@utwente.nl.

^{b)}Electronic mail: a.j.h.m.rijnders@utwente.nl.

using a KrF excimer laser with a fluence of 3 J/cm^2 on a stoichiometric LSMO target and a pulse repetition rate of 1 Hz. The target-substrate distance was 50 mm. The substrate temperature during deposition was $750 \text{ }^\circ\text{C}$ and the O_2 partial pressure was 0.35 mbar. Growth was monitored *in situ* with the high-pressure reflection high-energy electron diffraction (RHEED).⁹ Under these conditions, the deposition rate was 2 nm/min, estimated from the RHEED intensity oscillation during the initial 10 nm growth. After deposition, the samples were cooled to $600 \text{ }^\circ\text{C}$ in 0.35 mbar O_2 and subsequently to room temperature in 1 bar O_2 , at a rate of $10 \text{ }^\circ\text{C/min}$.

Substrate and film crystal lattice parameters and directions were determined from x-ray diffraction measurements. Usually torque measurements are used to determine the easy axis directions and the anisotropy strength. However such measurements did not provide conclusive information on the anisotropy in the thin films considered here, because the torque signal was swamped by the substrate signal.¹⁰ Instead we used magnetization measurements to determine the easy axis directions. Complete room temperature magnetic hysteresis loops (*MH*-loops) were measured as function of the applied in-plane magnetic field (*H*) (sweeping over $\pm 5000 \text{ Oe}$) using a vector vibrating sample magnetometer, allowing the simultaneous measurement of the magnetization parallel (M_{par}) and perpendicular (M_{perp}) to the applied field direction, both in the plane of the film. This allows the determination of the direction (angle φ_M with $[\bar{1}\bar{1}1]_o$) and magnitude of the total in-plane remanent magnetization vector $M_{r,\text{tot}}$ as function of φ_H . In zero field one expects $M_{r,\text{tot}}$ to be aligned with the in-plane projection of the magnetic easy axis. In that case φ_M can be identified with the direction of the (in-plane) magnetic easy axis (φ_{easy}). The large substrate signal was subtracted by fitting a linear $M(H)$ function at the raw high-field magnetization data, where the LSMO magnetization is constant. The Curie temperature T_c of all films is at least 360 K. No systematic dependence of T_c on film thickness is observed.

Figure 2 shows the measured remanent magnetization components $M_{r,\text{par}}(\varphi_H)$ and $M_{r,\text{perp}}(\varphi_H)$ of the various LSMO thin films. The films thinner than 200 nm show clear signatures of uniaxial anisotropy with 180° periodicity, which can approximately be described with $M_{r,\text{par}} \propto |\cos(\varphi_H - \varphi_{\text{easy}})|$, with φ_{easy} as the uniaxial easy axis direction. With increasing thickness the maxima in $M_{r,\text{par}}$ shift from about 15° to higher in-plane angles, the maxima decrease in height and for the thickest samples a secondary maximum appears at about 130° for the thickest samples. Note that the second maximum is not at a 90° angle with the main maximum. Further, in the hard axis direction at $\varphi_H \approx 105^\circ$ a discontinuity in the $M_{r,\text{par}}-\varphi_H$ curve is developing with increasing film thickness.

The discontinuous change in $M_{r,\text{perp}}$ at $\varphi_H \approx 105^\circ$ of the thinner films reflects the approximately 180° inversion of the direction of the magnetization vector along the easy axis, as seen in the φ_M versus φ_H graph. For the thicker films a second jump in $M_{r,\text{perp}}$ appears at $\varphi_H \approx 0^\circ$ and the changes in φ_M reduce from about 180° to about 90° . These jumps can be associated with the magnetic hard axis directions φ_{hard} . The hard axis *MH*-loop (not shown) of the thinnest samples (20–50 nm) shows the characteristics of a two-phase uniaxial sample, showing a straight line *MH*-dependence up to a critical field H_c , above which the domains form a single phase

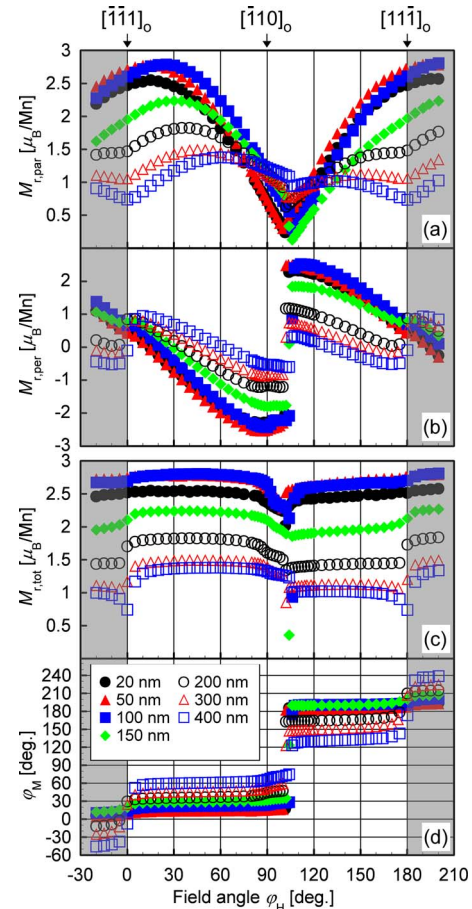


FIG. 2. (Color online) Field angle (φ_H) dependence of the parallel ($M_{r,\text{par}}$) (a) and perpendicular ($M_{r,\text{perp}}$) (b) component of the in-plane remanent magnetization vector, the total in-plane remanence ($M_{r,\text{tot}}$), and (c) the angle φ_M of (d) $M_{r,\text{tot}}$.

and rotate according to the Stoner–Wohlfahrt relations.¹¹ This allows the determination of the room temperature anisotropy constant, $K_u \approx 9.2 \text{ kJ/m}^3$. (For the thicker samples this analysis is not applicable, because the hard axis loops show some hysteresis).

The results may be interpreted as follows. In bulk LSMO (rhombohedral lattice structure) the $[111]_{\text{pc}}$ direction, corresponding to the longest body diagonal of the pseudocube, is the magnetic easy axis.^{12,13} In the $\{011\}_{\text{pc}}$ orientation discussed here, the in-plane projection of any body diagonal does not correspond to the magnetic easy axis direction found for the thinnest samples. We conclude that the magnetic anisotropy is not due to intrinsic magnetocrystalline anisotropy, but due to substrate induced strain anisotropy. For the thin films the magnetization is predominantly in-plane, due to the relatively strong demagnetization. (With saturation energy $M_s(300 \text{ K}) = 5.1 \times 10^5 \text{ A/m}$ the demagnetization energy for the film without out-of-plane domains is estimated as $E_d = 1.6 \times 10^5 \text{ J/m}^3$.) The decreasing in-plane $M_{r,\text{tot}}$ values with increasing film thickness indicate an increase in the out-of-plane component of the magnetization (M_z) with increasing thickness. This may be caused by an increase in the out-of-plane component of the easy axis, as well as by a decrease in the demagnetization energy due to domain formation and/or decreasing aspect ratio. In fact domain formation is strongly enhanced by the presence of an M_z component.¹⁴ Out-of-plane domains should not affect the

direction of the in-plane remanent magnetization components, thus one expects the in-plane component (here $M_{r,\text{tot}}$) to be predominantly aligned along the nearest in-plane easy axis. The maxima and minima in $M_{r,\text{par}}$ therefore correspond approximately to the in-plane easy and hard directions. The jumps in $M_{r,\text{perp}}$ can be associated with the angles at which the in-plane magnetization jumps between two easy axis directions. The easy axis directions must then be approximately in between these angles. The shift from a single jump in $M_{r,\text{perp}}$ (at $\varphi_{\text{hard1}} \approx 105^\circ$) for the thin samples to two jumps ($\varphi_{\text{hard2}} \approx 0^\circ$, respectively, $\varphi_{\text{hard1}} \approx 105^\circ$), for the thicker samples indicates the change from uniaxial to biaxial anisotropy. This is also reflected in the change of the 180° jumps in φ_M to approximately 90° jumps with increasing thickness.

We ascribe these features to the effects of a gradual structural change over the thickness of the film due to strain relaxation. This changes the relative strength of easy axis directions. It is noted that the surface unit cell of $\text{NGO}(112)_o$ is nonrectangular. For the thinnest films the (uniaxial) easy axis is predominantly in the $\text{NGO}[\bar{1}\bar{1}1]_o$ direction, but the magnetization vector is rotated slightly toward the long diagonal of the surface unit cell (in the $[02\bar{1}]_o$ direction). This suggests that the in-plane deformation of the surface unit cell plays an important role in the direction of the magnetic easy axis. XRD measurements show that the originally coherently strained thin LSMO film relaxes with increasing thickness. Films up to a thickness of 150 nm grow coherently with in-plane lattice parameters equal to the substrate lattice parameters, including the angle of 90.5° as shown in Fig. 1 and an out-of-plane lattice parameter of 0.552 nm. The high crystalline quality of the films is evidenced from the rocking curves of the $(224)_o$ peaks as well, which have a full width at half maximum (FWHM) of 0.05° . For the thicker films a part of the film remains coherent to the substrate and a part of the film relaxes to a structure with smaller out-of-plane and larger in-plane lattice parameters. For example the 100 nm LSMO film is still fully strained and shows the in-plane 90.5° angle of the surface unit cell, whereas the 400 nm film shows both the 90.5° angle as well as the relaxed angle of 90° . The rocking curves of the relaxed part of the thicker films have a FWHM of 0.7° , which shows that the crystalline quality decreases with film thickness.

In summary, we studied the in-plane magnetic anisotropy of $\{011\}_{\text{pc}}$ oriented LSMO thin films grown on $\text{NGO}(112)_o$. The $M_{r,\text{par}}-\varphi_H$ data show rotation of the magnetic easy axes with increasing film thickness. The in-plane magnetic anisotropy changes from uniaxial to biaxial as the film becomes thicker. This effect appears to be related to the gradual relaxation of the planar asymmetric distortion of the surface unit cell of the $\text{NGO}(112)_o$ with increasing film thickness, changing the crystal symmetry from monoclinic to orthorhombic. It is evident that to obtain a well-defined uniaxial anisotropy in electrodes of TMR junctions one has to use electrodes with a thickness less than 100 nm. In that case also most of the magnetization is in the plane of the film.

This work was supported by NanoNed, a nanotechnology program of the Dutch Ministry of Economic Affairs, the EU FP6 program NANOXIDE (NMP-2004-3.4.2.1-1) and a VIDI (G.R.) program of the Netherlands Organization for Scientific Research NWO.

- ¹Y. Tokura, A. Urushibara, Y. Moritomo, T. Arima, A. Asamitsu, G. Kido, and N. Furukawa, *J. Phys. Soc. Jpn.* **63**, 3931 (1994).
- ²A. Urushibara, Y. Moritomo, T. Arima, A. Asamitsu, G. Kido, and Y. Tokura, *Phys. Rev. B* **51**, 14103 (1995).
- ³J.-H. Park, E. Vescovo, H.-J. Kim, C. Kwon, R. Ramesh, and T. Venkatesan, *Nature (London)* **392**, 794 (1998).
- ⁴J. Z. Sun, W. J. Gallagher, P. R. Duncombe, L. Krusin-Elbaum, R. A. Altman, A. Gupta, Y. Lu, G. Q. Gong, and G. Xiao, *Appl. Phys. Lett.* **69**, 3266 (1996).
- ⁵M. Bowen, M. Bibes, A. Barthélémy, J.-P. Contour, A. Anane, Y. Lemaître, and A. Fert, *Appl. Phys. Lett.* **82**, 233 (2003).
- ⁶Y. Ishii, H. Yamada, H. Sato, H. Akoh, Y. Ogawa, M. Kawasaki, and Y. Tokura, *Appl. Phys. Lett.* **89**, 042509 (2006).
- ⁷H. Yamada, Y. Ogawa, Y. Ishii, H. Sato, M. Kawasaki, H. Akoh, and Y. Tokura, *Science* **305**, 646 (2004).
- ⁸Y. Mukunoki, N. Nakagawa, T. Susaki, and H. Y. Hwang, *Appl. Phys. Lett.* **86**, 171908 (2005).
- ⁹G. J. H. M. Rijnders, G. Koster, D. H. A. Blank, and H. Rogalla, *Appl. Phys. Lett.* **70**, 1888 (1997).
- ¹⁰K. Steenbeck, personal communication.
- ¹¹L. Néel, R. Pauthenet, G. Rimet, and V. S. Giron, *J. Appl. Phys.* **31**, S27 (1960).
- ¹²A. Khapikov, L. Uspenskaya, and I. Bdikin, *Appl. Phys. Lett.* **77**, 2376 (2000).
- ¹³M. Konoto, T. Kohashi, K. Koike, T. Arima, Y. Kaneko, Y. Tomioka, and Y. Tokura, *Appl. Phys. Lett.* **84**, 2361 (2004).
- ¹⁴S. Chikazumi, *Physics of Ferromagnetism* (Oxford University Press, Oxford, 1997).